lanesi, G. (1978), *Proc. Natl. Acad. Sci. U.S.A. 75,* 1126.
Sollner-Webb, B., and Felsenfeld, G. (1975), *Biochemistry 14,* 2915.
Sollner-Webb, B., Camerini-Otero, R. D., and Felsenfeld, G. (1976), *Cell 9,* 179.
Summers, W. C., and Szybalski, W. C. (1968), *Virology 34,* 9.
Van der Westhuyzen, D. R., and Von Holt, C. (1974), *Biochim. Biophys. Acta 359,* 341.
Weintraub, H., and Groudine, M. (1976), *Science 193,* 848.
Weintraub, H., and van Lente, E. (1974), *Proc. Natl. Acad. Sci. U.S.A. 71,* 4249.
Weintraub, H., Worcell, A., and Alberts, B. (1976), *Cell 9,* 409.
Yamamoto, K. R., Alberts, B. M., Benzinger, R., Lawhorne, L., and Treiber, G. (1970), *Virology 40,* 734.

Histone–Histone Interactions in a Lower Eukaryote, *Tetrahymena thermophila*†

Claiborne V. C. Glover and Martin A. Gorovsky*

ABSTRACT: The six pairwise interactions of *Tetrahymena* macronuclear histones H2A (formerly HX), H2B, H3, and H4 have been studied using the techniques of circular dichroism and continuous variation. Parallel experiments have been performed with calf thymus histones as controls, and the 12 possible interspecies pairs have also been examined. The behavior of three of the ciliate histones, H2A, H2B, and H3, is virtually identical with that of their vertebrate counterparts. *Tetrahymena* H4 exhibits a pattern of interactions identical with that of calf thymus H4, but displays significant quantitative differences in the strength of those interactions. Although we have not entirely eliminated the possibility that these differences may be artifactual, we suggest that they reflect the unique primary structure of *Tetrahymena* H4. These results extend the pattern of histone–histone interactions defined for plants, animals, and fungi to include the protists as well and imply the strong evolutionary conservatism of this pattern in spite of the electrophoretic and compositional differences which exist between homologous histones of different organisms. In addition, they demonstrate conclusively that histone HX should be redefined as *Tetrahymena* H2A.

Understanding of the subunit structure of chromatin has become increasingly more refined since the concept was first proposed (Kornberg, 1974). Genomes of higher eukaryotes appear to be organized in particulate structures approximately 100 Å in diameter containing 140 base pairs of DNA complexed with a protein octamer consisting of two each of the four inner histones H2A, H2B, H3, and H4 (for review, see Kornberg, 1977). An H3–H4 tetramer (the arginine-rich histone kernel) appears capable of organizing DNA in much the same manner as it is organized in the intact nucleosome (Sollner-Webb et al., 1976; Camerini-Otero & Felsenfeld, 1977) and presumably is of central importance to nucleosome structure. This hypothesis is supported by the profound evolutionary conservatism of these two proteins (DeLange et al., 1969; Patthy et al., 1973). Histone–histone interactions within the nucleosome have been explored using a variety of techniques, and it has been found that the pattern of interactions (for review, see Isenberg, 1977, 1978), like the histones themselves, has been highly conserved over evolutionary distances as great as those which separate animals (D'Anna & Isenberg, 1974b), plants (Spiker & Isenberg, 1977), and fungi (Mardian & Isenberg, 1978).

The ciliated protozoan, *Tetrahymena thermophila,* is a lower eukaryotic organism possessing two types of nuclei, a transcriptionally active macronucleus and a transcriptionally inactive micronucleus, the latter being responsible for genetic continuity of the species (Gorovsky, 1973). The chromatin of both nuclei exhibits typical periodic as well as particulate structure (Gorovsky et al., 1978), and the properties of *Tetrahymena* histones have been studied in some detail. Histones H1, H2B, H3, and H4 share extensive biochemical similarity with their vertebrate homologues, and only HX cannot be equated unambiguously with a vertebrate histone (Johmann & Gorovsky, 1976a).[1] Although all five histones are found in the macronucleus, we have been unable to demonstrate the presence of either H1 or H3 in the micronucleus (Gorovsky & Keevert, 1975).

The pattern of interactions exhibited by *Tetrahymena* histones has been investigated by electron microscopic analysis of nucleosomes reconstituted from three calf and one *Tetrahymena* histone (Gorovsky et al., 1978). By this assay, *Tetrahymena* H2B and H3 substitute efficiently for their vertebrate counterparts, while HX and H4 do not. These and other observations have led us to speculate on the possible existence of unique interactions among *Tetrahymena* histones, particularly between HX and H4, which might explain the formation of micronuclear nucleosomes in the absence of H3.

† From the Department of Biology, University of Rochester, Rochester, New York 14627. *Received June 20, 1978.* This research was supported by a grant from the U.S. Public Health Service (GM 21793). C. V. C. Glover is a U.S. Public Health Service, National Institutes of Health, Predoctoral Trainee and M. A. Gorovsky is a recipient of a U.S. Public Health Service, National Institutes of Health, Research Career Development Award.

[1] We have previously shown that a fraction formerly referred to as *Tetrahymena* HY is monoacetylated H2B (Johmann & Gorovsky, 1976a).

0006-2960/78/0417-5705$01.00/0

This report explores the pattern of interactions among *Tetrahymena* histones in greater detail, using the methods of circular dichroism and continuous variation (D'Anna & Isenberg, 1973). The results indicate that the pattern of interactions defined for histones of other eukaryotes can be extended to the histones of protozoa as well. In particular, *Tetrahymena* HX has properties which clearly identify it as *Tetrahymena* H2A. No unique pairwise interactions have been observed between the *Tetrahymena* histones. Surprisingly, however, quantitative differences between the behavior of calf and *Tetrahymena* H4's have been observed.

Materials and Methods

Histones. Macronuclei of *Tetrahymena thermophila* (formerly *T. pyriformis*), strain BVII, were isolated, and whole histone was extracted as previously described (Gorovsky et al., 1975). Histone H1 was removed by extraction with perchloric acid, and the inner histones were purified by a combination of exclusion and ion-exchange chromatography. Crude histone was dissolved in 0.01 N HCl, applied to a column of Bio-Gel P-60, and eluted in the same solvent. Fractions containing the lysine-rich pair H2A/H2B or the arginine-rich pair H3/H4 were pooled separately and applied to a column of carboxymethyl-cellulose (Cellex-CM, Bio-Rad Corp.) equilibrated in 0.01 N HCl. Each pair was eluted with a linear gradient of HCl from 0.01 to 0.025 N. The ion-exchange column removed remaining cross-contamination of the two pairs as well as most of the residual non-histone protein. Each histone pair was dialyzed 36 h against distilled, deionized water and lyophilized. The histones of each pair were subsequently separated by chromatography on Bio-Gel P-60 equilibrated in 0.04 N HCl, 0.1 M NaCl, and 0.02% NaN_3. The arginine-rich pair was reduced prior to application by incubation for 1 h at 40 °C in 1 mM Tris, pH 9.0, containing 8 M urea and a tenfold molar excess of DTT.[2] Appropriate fractions were pooled, dialyzed, and lyophilized as before and stored in a desiccator at 23 °C until used.

Calf thymus histone was obtained by homogenizing the tissue in 0.14 M NaCl–0.03 M $NaHSO_3$ and, after repeated washings of the homogenate, extracting the histones with 0.4 N H_2SO_4. Purified fractions were obtained using a combination of the three chromatographic systems described above.

Purity of all histone fractions was estimated by analytical gel electrophoresis. Histone cross-contamination was assayed on acetic acid–2.5 M urea gels (Panyim & Chalkley, 1969) and found to be below detectable levels for both calf thymus and *Tetrahymena*. Contamination with non-histone proteins was monitored on sodium dodecyl sulfate gels (Laemmli, 1970, as modified by Weintraub et al., 1975) and was less than 2% for all fractions except *Tetrahymena* H3 (<5%).

Stock solutions of individual histones were prepared at 2×10^{-5} M in water and stored in siliconized vials at −20 °C. Histone concentrations were estimated by absorbance measurements at 230 nm using a Gilford Model 2400 spectrophotometer. Proper calibration of both wavelength and absorbance was monitored periodically using appropriate standards. Molar extinction coefficients at 230 nm for calf thymus H2A, H2B, and H4 were taken as 4.3×10^4, 5.4×10^4, and 4.2×10^4 cm^{-1} M^{-1}, respectively (D'Anna & Isenberg, 1974a); and a value of 4.8×10^4 cm^{-1} M^{-1} was used for calf thymus H3 based on the absorption coefficient at 275.5 nm (D'Anna & Isenberg, 1974b) and the observed ratio of absorbance at 230 nm to that at 275.5 nm. Concentrations of *Tetrahymena* histones were determined initially on the basis of dry weight of the lyophilized powders, with moisture content being assumed equal to that of corresponding calf thymus histones, typically from 5 to 15%. Concentrations so obtained were converted to molarities on the basis of molecular weight estimates obtained by $NaDodSO_4$–polyacrylamide gel electrophoresis using calf thymus histones as standards. Although the apparent molecular weight of *Tetrahymena* H3 is 13 300 on Panyim & Chalkley $NaDodSO_4$ gels (Johmann & Gorovsky, 1976a), it is identical with that of calf thymus H3 on Laemmli–Weintraub $NaDodSO_4$ gels (Gorovsky & Bowen, unpublished observations). We chose the latter value in view of the strong evolutionary conservatism displayed by this protein. Molar extinction coefficients at 230 nm were subsequently determined and used routinely. Values of 4.3×10^4, 3.4×10^4, 4.8×10^4, and 4.2×10^4 cm^{-1} M^{-1} were obtained for *Tetrahymena* H2A, H2B, H3, and H4, respectively.

Since *Tetrahymena* H2A (HX) contains two primary sequence variants (Johmann & Gorovsky, 1976a), the H2A used in the experiments reported here is the natural 2:1 mixture of these two proteins having a weighted average molecular weight of 13 800.

Residue numbers of *Tetrahymena* histones were calculated from the molecular weight estimates; values obtained for H2A, H2B, H3, and H4 were 127, 123, 135, and 102 residues, respectively.

Circular Dichroism (CD). All measurements were made using a Jasco Model J-40 recording spectropolarimeter. The instrument was continuously flushed with nitrogen while in use and was calibrated daily with a solution of *d*-camphor-10-sulfonic acid. Data were collected at 23 °C unless otherwise noted. All measurements were made using a 2-mm pathlength cell and a total histone concentration of 10^{-5} M, giving a combined optical density for solute, solvent, plus cuvette not exceeding 1.0 at 205 nm. Continuous variation data were obtained at 220 nm; spectra were recorded from 245 to 205 nm. All CD measurements are reported either as $\Delta\epsilon$ in units of cm^{-1} M^{-1} of residue or as $\Delta\epsilon'$ in units of cm^{-1} M^{-1} of histone.

Solutions for CD were prepared by mixing histone stock solutions in water at 2×10^{-5} M, followed by dilution with an equal volume of either 0.02 N HCl or concentrated sodium phosphate buffer, pH 7.0. Histone mixtures containing H3 were incubated in the presence of DTT for 1 h at 40 °C before addition of salt or acid, and the final DTT concentration in these cases was 10^{-4} M. Mixtures for continuous variation experiments were made such that total histone concentration, C_0, remained constant at 10^{-5} M. When necessary, data were extrapolated to zero time of mixing in order to correct for histone self-aggregation.

Secondary structures of histones and histone complexes were estimated by the difference spectrum method of D'Anna & Isenberg (1972). The observed difference spectrum (spectrum in 0.01 or 0.02 M phosphate buffer minus spectrum in 0.01 N HCl) was compared with calculated difference spectra to estimate the relative proportions of α-helix and β-sheet structure induced by salt. Though this comparison is somewhat subjective, these proportions appeared to be close to 100% α helix and 0% β sheet for all cases not involving histone aggregation. The CD at 220 nm was then extrapolated to infinite phosphate to ensure the maximum number of molecules in the salt-induced conformation, and the percentage of residues undergoing random coil to α-helix transition was calculated from the following formula:

$$\frac{\Delta\epsilon_{220}(\text{sample}) - \Delta\epsilon_{220}(\text{random coil})}{\Delta\epsilon_{220}(\alpha\text{ helix}) - \Delta\epsilon_{220}(\text{random coil})} \times 100 \qquad (1)$$

[2] Abbreviations used: DTT, dithiothreitol; CD, circular dichroism; $NaDodSO_4$, sodium dodecyl sulfate.

TABLE I: Secondary Structure of *Tetrahymena* and Calf Thymus Histones at pH 7.0 and Infinite Phosphate Concentration.

histone/species		no. of residues	$\Delta\epsilon_{220}(\infty)^a$ (cm^{-1} M^{-1})	$\Delta\epsilon_{220}(R)^b$ (cm^{-1} M^{-1})	% α helix[c]	no. residues in α helix
H2A	Tet	127	1.91	1.22	7	9
	CT	129	2.04	0.99	11	14
H2B	Tet	123	1.81	0.76	11	13
	CT	125	2.24	0.66	16	20
H3	Tet	135	2.07	1.10	10	14
	CT	135	2.04	1.19	9	12
H4	Tet	102	1.18	0.53	6	6
	CT	102	1.47	0.57	9	9

[a] Circular dichroism at infinite phosphate concentration is estimated from a plot of $\Delta\epsilon_{220}$ vs. $1/[P]$ by extrapolation. [b] Circular dichroism of the random coil form is taken as the CD at 220 nm of histone dissolved in 0.01 N HCl. [c] Percentage of α helix is calculated using eq 1 of Materials and Methods.

The α-helix reference spectrum chosen was that of poly(L-lysine) (Greenfield & Fasman, 1969) for which $\Delta\epsilon_{220} = 10.70$ cm^{-1} M^{-1} residue, while the histone or histone mixture in 0.01 N HCl was taken as the random coil reference. Because of the subjectivity involved in determining the proportions of α helix and β sheet and the necessarily arbitrary choice of appropriate reference spectra, the results obtained with the method are presented more for their relative than for their absolute values.

A computer simulation of continuous variation experiments was designed in order to assess the effects of changes in association constant, molar CD of histones and complexes, histone concentration errors, etc. The simulation was based on the following assumptions: two species, A and B, interact to form a dimer, C; the equilibrium constant for the association is K; and the molar CD constants of the three components are E_A, E_B, and E_C, respectively. The initial concentrations, A_0 and B_0, are allowed to vary such that their sum, C_0, remains constant. The three equations:

$$A_0 = A + C \quad (2)$$

$$B_0 = B + C \quad (3)$$

$$K = C/(AB) \quad (4)$$

are solved for the three unknown concentrations, A, B, and C. Observed molar CD is then obtained from the relation:

$$E(K,E_C) = [E_A A(K) + E_B B(K) + E_C C(K)]/C_0 \quad (5)$$

Since A_0 and B_0 are known and E_A and E_B may be measured directly, E depends on two parameters, K and E_C. An analogous simulation may be derived for the case of tetramer formation.

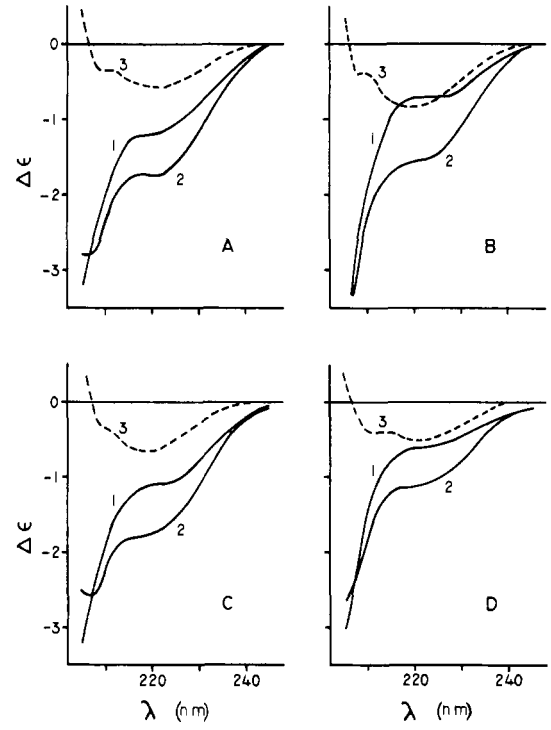

FIGURE 1: Circular dichroism spectra of *Tetrahymena* histones in 0.01 N HCl (curve 1) and in sodium phosphate buffer, pH 7.0 (curve 2). (A) H2A; (B) H2B; (C) H3; and (D) H4. Histone concentration was 10^{-5} M, and all measurements were made using a 2-mm pathlength cell. Phosphate concentration was 0.01 M for H2A, H2B, and H3, 0.02 M for H4. The phosphate spectrum of H3 was obtained at 4 °C in order to inhibit the rapid self-aggregation of this histone. Other spectra were obtained at 23 °C. The difference spectrum (curve 3) was calculated in each case by subtracting curve 1 from curve 2.

Results

Circular Dichroism of Individual Histones. The circular dichroism spectra of *Tetrahymena* histones (Figure 1) are qualitatively similar to those of calf thymus and pea histones, whether the spectra are obtained in 0.01 N HCl or in sodium phosphate buffer, pH 7. We have used the spectrum of each histone in 0.01 N HCl as the random coil reference for that histone and have used a difference spectrum method (see Materials and Methods) to estimate the kinds and amounts of secondary structure induced by salt. The difference spectrum in each case implies a random coil to 100% α-helix transition for some number of residues. After extrapolation of the data obtained at 220 nm to infinite salt concentration, the actual percentage of residues undergoing the transition is calculated as described in Materials and Methods. The results are given in Table I along with values obtained in our laboratory for calf thymus histone. With the exception of H3, the values obtained for *Tetrahymena* histones tend to be significantly less than those of corresponding calf thymus histones. In the case of *Tetrahymena* H2A closer examination of the data suggests that this protein has residual secondary structure even in 0.01 N HCl. Addition of salt then leads to only a slight increase in α-helix content because the molecule is already partially folded. *Tetrahymena* H2B and H4, by contrast, appear to be fully unfolded in 0.01 N HCl, suggesting either that these histones may renature less readily than their calf thymus homologues or that fewer residues adopt an α-helical conformation upon renaturation. These conclusions should be re-

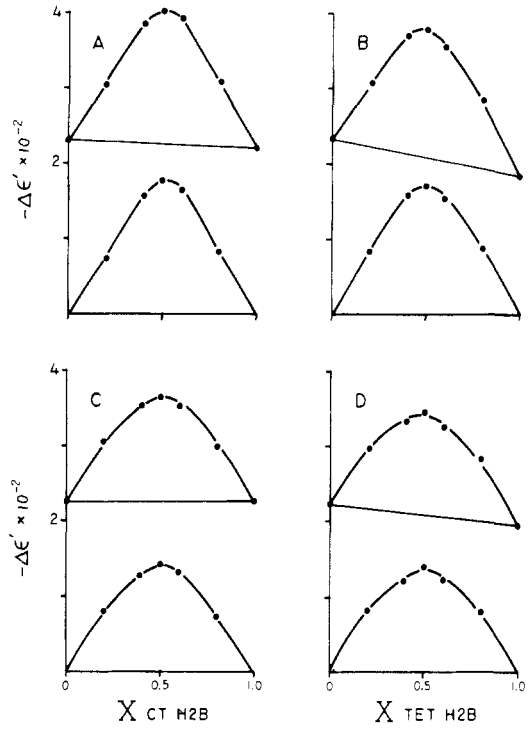

FIGURE 2: Continuous variation curves obtained for inter- and intraspecies mixtures of *Tetrahymena* and calf thymus histones H2A and H2B in 0.01 M sodium phosphate buffer, pH 7.0. (A) CT H2A-CT H2B; (B) CT H2A-Tet H2B; (C) Tet H2A-CT H2B; and (D) Tet H2A-Tet H2B. Circular dichroism at 220 nm is plotted vs. mole fraction of H2B. Expected values were calculated for mixtures of noninteracting histones by linear interpolation and subtracted from the observed value at each point, yielding the curve shown in the lower half of each panel. Total histone concentration, C_0, was 10^{-5} M, and all measurements were made at 23 °C using a 2-mm pathlength cell.

garded cautiously, however, since the data will also reflect any errors made in the estimation of histone concentrations.

Tetrahymena H3 and H4, like the arginine-rich histones of higher eukaryotes, exhibit time-dependent changes in circular dichroism under proper conditions of concentration, pH, temperature, and ionic strength. When incubated at 10^{-5} M at 23 °C in 0.01–0.05 M phosphate, pH 7.0, each of the histones displays a gradual increase in CD at 220 nm (data not shown). This increase is accompanied by changes at other wavelengths, and the spectrum of each histone at 24 h indicates that considerable β-sheet structure has formed. In the case of calf thymus H3 and H4 such behavior (designated the slow step) has been correlated directly with the self-aggregation of these proteins (D'Anna & Isenberg, 1974b). The similar behavior of *Tetrahymena* H3 and H4 probably reflects a similar self-aggregation, though light scattering studies are required to demonstrate this conclusively. While the slow step of *Tetrahymena* H3 closely resembles that of its mammalian homologue, that of *Tetrahymena* H4 does not: both the rate and the final extent of the slow step are reduced relative to calf thymus H4. *Tetrahymena* H2A, like the lysine rich histones of calf thymus, displays no detectable slow step over a period of at least 24 h (conditions as above). While this result does not preclude the self-aggregation of this histone, it is consistent with the minimal self-aggregation observed for the lysine-rich histones of other species. Surprisingly, *Tetrahymena* H2B does exhibit a time-dependent increase in CD at 220 nm (10^{-5} M, 23 °C, 0.05 M phoshate). Although less extensive than that of the arginine rich histones, the slow step of *Tetrahymena* H2B is accompanied by similar β-sheet formation and may well reflect the self-aggregation of this histone. Since *Tetrahymena* H2B appears to be functionally equivalent to calf H2B (see below), the phenomenon of self-aggregation may be more incidental than integral to the function of histone proteins.

Pairwise Interactions. We have examined the pattern of pairwise interactions among the four *Tetrahymena* histones by the method of continuous variation using circular dichroism at 220 nm as an assay. In all cases the homologous pair of calf thymus histones has served as standard, and our results with the latter proteins are consistent with those of D'Anna & Isenberg (1974b). In parallel with the intraspecies pairs, we have also examined the 12 potential interspecies interactions involving one calf and one *Tetrahymena* histone. No histone–histone interactions are observed in 0.01 N HCl, but the addition of salt at pH 7.0 leads to the formation of a number of complexes detectable by CD.

H2A–H2B: Continuous variation curves for the four possible H2A–H2B interactions are presented in Figure 2. The strong interaction detectable by CD for the lysine-rich pair of calf (Figure 2A) is observed for *Tetrahymena* H2A and H2B as well (Figure 2D). Although the curves for the two intraspecies interactions are remarkably similar, they do exhibit slight differences in both shape and peak height. These differences could be ascribed entirely to H2A, entirely to H2B, or partly to both. We have performed continuous variation experiments for the two possible interspecies interactions in order to distinguish among these alternatives. Figures 2B and 2C show continuous variation curves obtained for interactions between calf H2A and *Tetrahymena* H2B and between *Tetrahymena* H2A and calf H2B, respectively. Comparison of these curves with those for the intraspecies complexes demonstrates that the interactions of *Tetrahymena* H2B are indistinguishable by CD from those of calf thymus H2B (Figure 2, compare A with B and C with D), while the interactions of *Tetrahymena* H2A are slightly but consistently diminished relative to those of its mammalian counterpart (compare A with C and B with D). Thus, differences in H2A alone can account for the slight differences observed between the two intraspecies interactions. Relative to those involving calf H2A, interactions involving *Tetrahymena* H2A appear to display a small reduction in either the association constant for interaction, the secondary structure induced by complexing, or both. Until preparative methods for the separation of the two parental species of *Tetrahymena* H2A are developed, we cannot be certain whether this behavior is representative of both sequence variants or whether the continuous variation curves actually reflect an average of two distinct interactions, one stronger and perhaps identical with those involving calf thymus H2A and one weaker. Nevertheless, to a first approximation, the behavior of *Tetrahymena* H2A, like that of *Tetrahymena* H2B, is strikingly similar to that of its mammalian counterpart.

The stoichiometry of each complex in Figure 2 appears to be 1:1, as evidenced by the location of the curve maximum in each case at a mole fraction of approximately 0.5 (D'Anna & Isenberg, 1973). This result implies complexes of the general form A_nB_n, where n is an integer. D'Anna & Isenberg (1974a) have suggested on the basis of equilibrium sedimentation analysis that the calf thymus H2A–H2B complex is a dimer ($n = 1$). Consideration of the probable value of n for the remaining complexes of Figure 2 is deferred until the Discussion.

The secondary structure present in the H2A–H2B complexes can be estimated by the difference spectrum method. In each case the difference spectrum is characteristic of random coil to α-helix transition for some number of residues, the actual number of which is estimated by extrapolating the CD

TABLE II: Secondary Structure of Inter- and Intraspecies Complexes of *Tetrahymena* and Calf Thymus Histones at pH 7.0 and Infinite Phosphate Concentration.

complex	no. of residues[a]	$\Delta\epsilon_{220}(\infty)$[b] ($cm^{-1}$ M^{-1})	$\Delta\epsilon_{220}(R)$[c] (cm^{-1} M^{-1})	% α helix,[d] minimum	no. of residues in α helix, minimum	calcd no. residues in α helix, noninteracting mixture	α-helix formation upon complexing,[f] minimum
CT H2A/CT H2B	254	3.39	0.83	26	66	34	32
CT H2A/Tet H2B	252	3.25	0.86	24	61	27	34
Tet H2A/CT H2B	252	3.13	0.90	23	57	29	28
Tet H2A/Tet H2B	250	3.02	1.03	21	52	22	30
CT H4/CT H2B	227	3.00	0.60	24	54	29	25
CT H4/Tet H2B	225	2.68	0.71	20	44	22	22
Tet H4/CT H2B	227	2.04	0.56	15	33	26	7
Tet H4/Tet H2B	225	1.89	0.60	13	29	19	9
CT H4/CT H3	474	2.24	0.95	13[e]	62[e]	42	20[e]
CT H4/Tet H3	474	2.24	0.90	14[e]	64[e]	45	19[e]
Tet H4/CT H3	474	1.97	0.97	10	49	37	12
Tet H4/Tet H3	474	1.98	0.90	11	52	40	12

[a] All calculations assume that H2A-H2B and H4-H2B complexes are dimers, H4-H3 complexes, tetramers. See Discussion. [b] Circular dichroism at infinite phosphate concentration is estimated from a plot of $\Delta\epsilon_{220}$ vs. $1/[P]$ by extrapolation. [c] Circular dichroism of the random coil form is taken as the CD at 220 nm of histone dissolved in 0.01 N HCl. [d] Percentage of α helix is calculated using eq 1 of Materials and Methods. [e] Values are best rather than minimum estimates. See text. [f] Values for calf thymus are substantially larger than those reported by D'Anna & Isenberg (1974), presumably because our data were extrapolated to infinite phosphate concentration at $C_0 = 10^{-5}$ M rather than at $C_0 = 0.5 \times 10^{-5}$ M.

at 220 nm to infinite phosphate, as for the individual histones (Table II). The results so obtained are actually minimum estimates of the true values since even at infinite phosphate the complexes are in equilibrium with histone monomers. Ideally, E_C (as defined in Materials and Methods) should be extrapolated to infinite phosphate, but, as detailed in the Discussion, this parameter is difficult to determine with confidence. It is clear, nonetheless, that complexing leads to additional secondary structure in the participating histones beyond that which they possess separately (see last column of Table II); it is this additional structure which allows detection of the complexes by CD.

H4-H2B: Figure 3 shows continuous variation curves obtained for each of the four H4-H2B pairs. Like the corresponding calf pair (Figure 3A), *Tetrahymena* H2B and H4 interact to form a complex (Figure 3D) which is detectable by circular dichroism at 220 nm. However, in this case, the magnitude of the interaction for *Tetrahymena* histones is substantially diminished relative to the interaction for calf histones. The interspecies interactions again identify which histone(s) is (are) responsible for the differences observed between the two intraspecies interactions. As was the case for its interactions with H2A, the interactions of *Tetrahymena* H2B with both calf and *Tetrahymena* H4 are indistinguishable from corresponding interactions of calf H2B (Figure 3, compare A with B and C with D). Thus, not only does ciliate H2B exhibit both of the strong interactions displayed by mammalian H2B, but within the resolution of our techniques the behavior of the two homologues is virtually identical. In contrast, the behavior of *Tetrahymena* H4 differs significantly from that of its mammalian counterpart, whether interacting with calf H2B (compare A with C) or *Tetrahymena* H2B (compare B with D). In both cases, the association constant and/or the additional secondary structure formed upon complexing are substantially reduced for *Tetrahymena* H4 relative to calf H4. The latter result holds over a substantial range of phosphate concentration (0.0031-0.02 M) and is not confined to a single preparation of *Tetrahymena* H4. Hence, differences between calf and *Tetrahymena* H4 can account completely for the differences observed between the two intraspecies interactions.

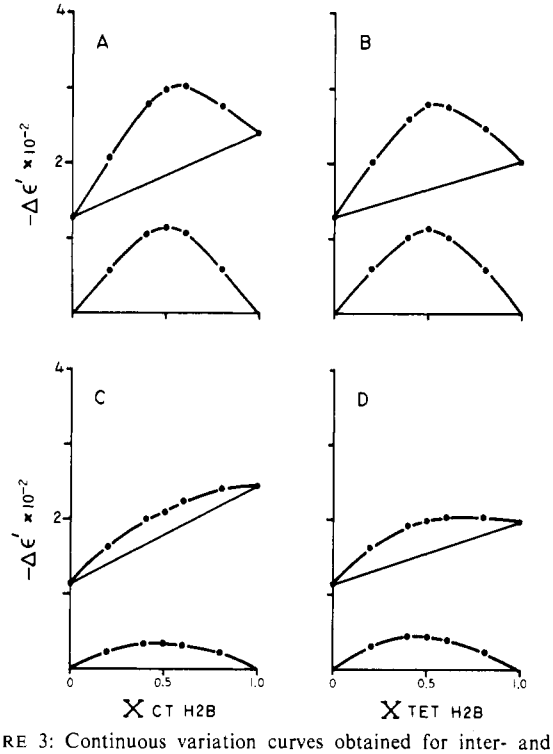

FIGURE 3: Continuous variation curves obtained for inter- and intraspecies mixtures of *Tetrahymena* and calf thymus H4 and H2B in 0.02 M sodium phosphate buffer, pH 7.0. (A) CT H4-CT H2B; (B) CT H4-Tet H2B; (C) Tet H4-CT H2B; and (D) Tet H4-Tet H2B. Circular dichroism at 220 nm is plotted vs. mole fraction of H2B. Expected values were calculated for mixtures of noninteracting histones by linear interpolation and subtracted from the observed value at each point, yielding the curve shown in the lower half of each panel. Total histone concentration, C_0, was 10^{-5} M, and all measurements were made at 23 °C using a 2-mm pathlength cell.

All of the H4-H2B complexes exhibit approximately 1:1 stoichiometries. Difference spectra for these complexes suggest

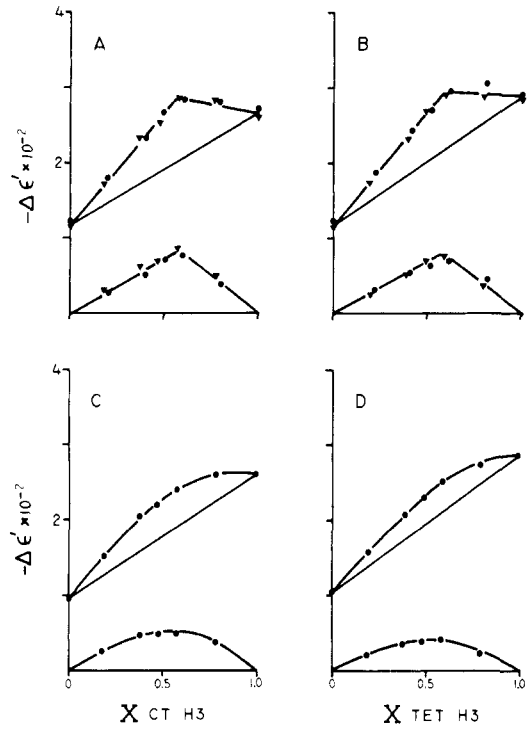

FIGURE 4: Continuous variation curves obtained for inter- and intraspecies mixtures of *Tetrahymena* and calf thymus H4 and H3 in 0.01 M sodium phosphate buffer, pH 7.0. (A) CT H4–CT H3; (B) CT H4–Tet H3; (C) Tet H4–CT H3; and (D) Tet H4–Tet H3. Circular dichroism at 220 nm is plotted vs. mole fraction of H3. Expected values were calculated for mixtures of noninteracting histones by linear interpolation and subtracted from the observed value at each point, yielding the curve shown in the lower half of each panel. Total histone concentration, C_0, was 10^{-5} M, and all measurements were made at 23 °C using a 2-mm pathlength cell. Triangular symbols in A and B represent data from a second experiment performed under identical conditions.

that the secondary structure induced by salt is primarily α helix and that it is greater for histones in complexes than for histones separately. Minimum estimates of the α-helical content of H4–H2B complexes are given in Table II.

H4–H3: Continuous variation curves for the four possible H4–H3 interactions are presented in Figure 4. *Tetrahymena* H4 and H3, like their calf thymus homologues, interact to form a complex which is detectable by circular dichroism. However, as for the H4–H2B interactions, the interaction between *Tetrahymena* H3 and H4 (Figure 4D) is significantly diminished relative to that between calf H3 and H4 (Figure 4A). Examination of the interspecies interactions indicate that the behavior of ciliate H3 closely resembles that of mammalian H3 (Figure 4, compare A with B and C with D), and that differences in H4 alone can completely account for differences between the intraspecies interactions (compare A with C and B with D). Since the continuous variation curves in panels A and B are triangles while those in C and D are arcs, it is apparent that H3 complexes involving *Tetrahymena* H4 have a reduced association constant relative to those involving calf H4. Whether or not there are also differences in the secondary structure of the complexes is uncertain.

The stoichiometry of the H4–H3 complexes is approximately 1:1. Although the curve maximum for both interactions involving calf H4 (Figures 4A and 4B) occurs at mole fraction H3 = 0.58, indicating an unusual stoichiometry, it is well documented that the calf complex is a tetramer (Kornberg, 1974; D'Anna & Isenberg, 1974b). The asymmetry in these continuous variation curves, therefore, probably reflects an error in estimation of histone concentration.

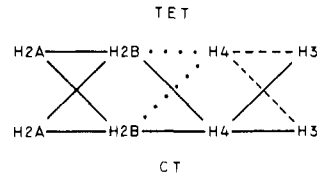

FIGURE 5: Summary of inter- and intraspecies pairwise interactions of the inner histones of *Tetrahymena* and calf thymus observed by circular dichroism of continuously varied mixtures. Solid lines denote strong interactions. Dashed or dotted lines denote interactions of *Tetrahymena* H4, which, though still strong, are diminished relative to those observed for calf thymus H4. Interactions other than those depicted are possible but could not involve formation of additional secondary structure in the complexed state.

The α-helical content of H4–H3 complexes is given in Table II. Since the continuous variation curves for the interactions involving calf H4 are sharply triangular (Figures 4A and 4B), the association constant must be large. Furthermore, since K is large, the curve maximum may be taken as a direct measurement of the CD of the complex. Thus, the α-helical contents reported for these two complexes containing calf H4 are best rather than minimum estimates.

H2A–H4: D'Anna & Isenberg (1974a) have reported a weak interaction between H2A and H4 from calf thymus. This interaction is demonstrable by circular dichroism at $C_0 = 3 \times 10^{-5}$ M and 0.0067 M phosphate, but the continuous variation curve deviates only slightly from that predicted for a mixture of noninteracting proteins. We have performed continuous variation experiments for the four possible H2A–H4 pairs (data not shown). In 0.02 M phosphate at $C_0 = 10^{-5}$ M, none of the curves departs more than 7% from the values predicted for noninteracting proteins. Therefore, these data offer no support for the hypothesis that there is a unique H2A–H4 interaction in *Tetrahymena* which might be correlated with the absence of H3 in the micronucleus.

Finally, we have sought interactions among the remaining possible pairs of histones, H2A–H3 and H2B–H3. Continuous variation curves obtained for all eight pairs at $C_0 = 10^{-5}$ M in 0.01 M phosphate are essentially identical with those predicted from simple additivity (data not shown). Circular dichroism thus offers no evidence for these interactions.

In summary, the behavior of ciliate H2A, H2B, and H3 is strikingly similar by these methods to that of their corresponding calf thymus homologues. In contrast, *Tetrahymena* H4, although qualitatively similar to calf H4 in that it interacts strongly both with H2B and with H3, is quantitatively dissimilar in that these interactions occur at only 25% (H2B) to 50% (H3) of the levels observed with mammalian H4. It is worth stressing that the interaction of *Tetrahymena* H4 with *Tetrahymena* and calf histones is similar; *Tetrahymena* H4 displays no obvious preference for *Tetrahymena* histones as partners.

Discussion

The behavior of *Tetrahymena* histones as studied by circular dichroism and the method of continuous variation is remarkably similar to that of corresponding calf, pea, or yeast histones. Thus, a similar pattern of pairwise histone–histone interactions has now been observed in each of the four eukaryotic kingdoms: animals, plants, fungi, and protists (Whittaker, 1969). In particular, this pattern has now been shown to apply to unicellular as well as multicellular eukaryotes. Figure 5 summarizes the interactions observed for *Tetrahymena* and calf histones using circular dichroism.

For each of the continuous variation curves shown in Figures 2–4, we have attempted to determine the equilibrium constant

for the interaction (K) and the molar circular dichroism of the complex (E_C) by obtaining a least-squares fit of eq 5 (see Materials and Methods) to the observed data. While in theory it is possible to extract both K and E_C, we find that, in practice, because of the noise present in our data, these parameters cannot be determined unambiguously. In some cases, grossly differing pairs of values for E_C and K yield equivalent approximations. These uncertainties in our estimates of K are sufficiently large to impair their usefulness even when advantage is taken of the observation that the free energy change associated with interaction is a logarithmic function of K (Spiker & Isenberg, 1978). It follows that, although we can be certain when two interactions differ (e.g., Figure 3A vs. Figure 3C), usually we cannot be certain whether K, E_C, or both have changed. Likewise, when two interactions are indistinguishable (e.g., Figures 3A and 3B), we cannot be certain that K and E_C for the two complexes are the same since an increase in one parameter may be offset by a corresponding decrease in the other. Of course, the simplest explanation in the latter case is that whatever the values of K and E_C they are the same or nearly so for both complexes.

The stoichiometry of each complex shown in Figures 2-4 appears to be 1:1, implying complexes of the general form A_nB_n with n an integer. Since the detailed shape of a continuous variation curve is a function of n, it is possible, in theory, to determine this parameter from such data. In practice, however, calculated curves for $n = 1$ (dimer) and $n = 2$ (tetramer) differ by less than the noise inherent in our measurements. We have not analyzed our complexes by high speed equilibrium sedimentation because of limitations in the amounts of purified *Tetrahymena* histones available for study. Therefore, the values of n for our complexes can only be inferred by analogy with corresponding calf complexes. This argument would appear to be soundest for those interspecies complexes which are identical with homologous calf complexes. Thus, we think it likely that the *Tetrahymena* H4-H3 complex is a tetramer while H4-H2B and H2A-H2B are dimers. These assignments are supported in part by unpublished observations that *Tetrahymena* H4-H3 and H2A-H2B complexes prepared by the method of van der Westhuyzen & von Holt (1971) elute from molecular exclusion columns at positions which are indistinguishable from corresponding calf thymus complexes (Gorovsky & Bowen, unpublished observations).

Heretofore, we have been unable to equate *Tetrahymena* HX with any vertebrate histone. The studies described here clearly demonstrate that *Tetrahymena* HX has properties which warrant its being renamed H2A. This histone interacts not only with *Tetrahymena* H2B but with calf thymus H2B as well. Furthermore, H2B is the *only* histone with which it displays a strong CD interaction. This pattern of histone-histone interactions is characteristic of H2A and of no other histone. An analogous identification of pea H2A has been made on the basis of its pattern of interactions with other histones (Spiker & Isenberg, 1977). Of course, it is still possible that *Tetrahymena* H2A has unique properties. It exhibits an evolutionary conservatism not found in vertebrate H2A's (Johmann & Gorovsky, 1976b), and also fails to reconstitute efficiently with calf thymus H2B, H3, and H4 as assayed by electron microscopy (Gorovsky et al., 1978). Whether this failure is due to steric packing difficulties with either or both of the H2A species or to the failure of other histone-histone interactions so far not characterized or to some other factor is not known.

The existence of a unique H2A-H4 interaction in *Tetrahymena* which might explain the absence of H3 in the micronucleus has not been substantiated by these studies. However, the method of continuous variation can only demonstrate, it cannot rule out, the existence of protein-protein interactions. Indeed, D'Anna & Isenberg (1974b) have shown that calf thymus H2A and H3 form a complex detectable by fluorescence anisotropy but not by circular dichroism. The failure to observe the complex by CD only implies that the secondary structure present in the complexed histones is not detectably different from that found in the noncomplexed histones. Thus, although we now regard the existence of a unique H2A-H4 interaction in *Tetrahymena* as unlikely, we cannot yet rule it out entirely.

The interaction of *Tetrahymena* H2B with both H2A and H4 is qualitatively and quantitatively similar to that of calf thymus H2B, strongly suggesting a highly conserved tertiary structure for this histone. This conclusion is entirely consistent with the results of nucleosome reconstitution studies reported previously (Gorovsky et al., 1978) which demonstrate that *Tetrahymena* H2B can interact with the other three calf inner histones to form nucleosomes.

It is interesting to speculate whether the sites of interaction for H2A and H4 on the H2B molecule are independent. Since only pairwise interactions have so far been studied, circular dichroism data are not informative on this point. However, in vivo cross-linking studies (Martinson & McCarthy, 1976) have demonstrated that H2B has at least two distinct binding sites, one for H2A and one for H4. While it is possible that H2A and H4 are competing for the same site on H2B under conditions used for CD, it seems more likely that the two sites are separate and correspond to those defined by cross-linking. We would then predict that H2B can form both complexes simultaneously in dilute phosphate, and we plan to explore this possibility by studying the appropriate three-histone mixture.

The equivalence of ciliate H3 and mammalian H3 in the studies reported here also was anticipated on the basis of nucleosome reconstitution experiments (Gorovsky et al., 1978). This equivalence remains somewhat startling, however, in view of the apparent structural uniqueness of ciliate H3. Although H3's from different species of *Tetrahymena* (like different vertebrate H3's) are electrophoretically indistinguishable, the electrophoretic mobility of *Tetrahymena* H3 has been shown to differ from that of calf thymus H3 on both acetic-urea and on $NaDodSO_4$-polyacrylamide gels (Johmann & Gorovsky, 1976a,b). The amino acid compositions of the two proteins differ, and a comparison of one-dimensional peptide maps indicates substantial differences between the primary sequences of the two histones (Glover & Gorovsky, unpublished observations). Since the sequence of H3 has become virtually fixed among higher eukaryotes (only 4 conservative substitutions distinguish the molecules from calf and pea; Patthy et al., 1973), it seems puzzling that a substantially different molecule from the lower eukaryotes apparently can substitute for it so effectively. Perhaps our assays for successful histone-histone interactions (CD) or for successful nucleosome reconstitution (electron microscopy) are too crude; more sensitive techniques might reveal that ciliate H3 fails in some important way to function properly in a higher eukaryotic nucleosome. Alternatively, H3 may serve more than a structural role in nucleosomes, and perhaps some other function, such as interaction with non-histone protein(s) peculiar to metazoans, cannot be fulfilled by ciliate H3. If the latter is the case, comparison of the primary sequences of calf and *Tetrahymena* H3 might reveal two distinct types of regions, conservative and variable. It is also possible that alterations in the sequence of *Tetrahymena* H3 are conservative and not grossly outside the variation which may be observed among higher eukaryotes. Thus, determination of the primary sequence of *Tetrahymena* H3 may

reveal a great deal about the role of H3 in chromatin structure and function.

Mardian & Isenberg (1978) have reported that the complex formed by yeast H3 with yeast H4 is not observable by circular dichroism, presumably because yeast H3 alone is already fully folded. We note that, in this respect, *Tetrahymena* resembles higher eukaryotes (calf and pea) rather than yeast: the CD behavior of yeast H3 so far remains unique.

The behavior of *Tetrahymena* H4 in the circular dichroism studies reported here parallels that of calf thymus H4 qualitatively but not quantitatively. The reduced efficiency with which *Tetrahymena* H4 forms complexes both with H2B and with H3 is consistent with its failure to substitute for calf thymus H4 in nucleosome reconstitution experiments and may explain our inability to reconstitute nucleosomes using *Tetrahymena* histones alone (Gorovsky et al., 1978). Since histone H4 is the most highly conserved protein known (DeLange et al., 1969), the simplest explanation for these results is that the molecule has been damaged during its purification. Spiker & Isenberg (1977) have shown that oxidation of methionine to methionine sulfoxide can interfere with formation of some histone–histone complexes. Although this type of damage has been associated with polyacrylamide gel electrophoresis (Alfageme et al., 1974), a step not involved in the purification of *Tetrahymena* H4, we nevertheless considered this possibility, especially since our (unpublished) observations indicate that *Tetrahymena* H4 has a second methionine in addition to that at position 84. This explanation is eliminated, however, by the observation that cyanogen bromide, which does not attack methionine sulfoxide (Gross, 1967), cleaves at least 80% of the methionine bonds in *Tetrahymena* H4. This figure is comparable to that obtained in our hands for calf H4 and for the other histones. Isenberg (1978) has suggested that deamidation of glutamine or asparagine residues may become significant under the acid conditions used for extraction and purification of histones. This or other types of structural damage have not yet been eliminated as possibilities. However, as noted previously (Gorovsky et al., 1978), calf thymus H4, when isolated by the procedures we use for *Tetrahymena* histones, functions normally in nucleosome reconstitution experiments.

Alternative explanations for the unusual behavior of *Tetrahymena* H4 require that its covalent structure differ substantially from that of calf or pea H4. We have sequenced more than 60 of the 102 residues of *Tetrahymena* H4 (Glover & Gorovsky, manuscript in preparation) and have found a minimum of 15 differences between the *Tetrahymena* and calf (or pea) sequences. Many of these differences involve nonconservative amino acid replacements. Furthermore, the degree of acetylation of specific lysine residues in *Tetrahymena* H4 differs from that observed for calf thymus H4. Finally, the N terminus itself is not acetylated as it is in higher eukaryotic H4's. Thus, it seems likely that the behavior of ciliate H4 reflects the unusual structure of this histone: either the molecule fails to renature properly under conditions suitable for calf H4 (which would be consistent with the data of Table I) or else it has innately weaker interactions with both H2B and H3. We favor the latter interpretation in view of our (unpublished) observations that, when trace amounts of [^{3}H]lysine labeled *Tetrahymena* macronuclei are mixed with calf thymus nuclei and extracted and analyzed by the method of van der Westhuyzen & von Holt (1971), *Tetrahymena* H3, but not H4, is found associated with the calf H3–H4 tetrameric complex (Gorovsky & Bowen, unpublished observation). Thus, the behavior of H4 in this experiment, which does not involve acid extraction, is completely consistent with the data presented in Figure 4 which indicate that *Tetrahymena* H4 has a lower affinity for *Tetrahymena* (or calf) H3 than does calf H4.

We wish to emphasize again that, although no interactions other than those depicted in Figure 5 were observed, others are still possible. Such interactions, if they exist, must be demonstrated by different techniques.

In summary, the pattern of histone–histone interactions defined for multicellular eukaryotes, plant, animal, and fungal, has been shown to extend (with only quantitative alterations) to unicellular eukaryotes as well. For H2B and H3 the similarities between *Tetrahymena* and calf histones are so strong that interkingdom complexes involving these histones are indistinguishable by CD from the appropriate intraspecies complexes. These observations reflect the powerful evolutionary restraints acting to conserve the structure and function of the inner histones.

Acknowledgments

We thank Dr. Douglas Turner for the use of his Jasco CD recorder. We also wish to acknowledge the excellent assistance of Josephine Bowen in the preparation of nuclei and histone.

References

Alfageme, C. R., Zweidler, A., Mahowald, A., & Cohen, L. H. (1974) *J. Biol. Chem. 249,* 3729.

Camerini-Otero, R. D., & Felsenfeld, G. (1977) *Nucleic Acids Res. 4,* 1159.

D'Anna, J. A., Jr., & Isenberg, I. (1972) *Biochemistry 11,* 4017.

D'Anna, J. A., Jr., & Isenberg, I. (1973) *Biochemistry 12,* 1035.

D'Anna, J. A., Jr., & Isenberg, I. (1974a) *Biochemistry 13,* 2098.

D'Anna, J. A., Jr., & Isenberg, I. (1974b) *Biochemistry 13,* 4992.

DeLange, R. J., Fambrough, D. M., Smith, E. L., & Bonner, J. (1969) *J. Biol. Chem. 244,* 5669.

Gorovsky, M. A. (1973) *J. Protozool. 20,* 19.

Gorovsky, M. A., & Keevert, J. B. (1975) *Proc. Natl. Acad. Sci. U.S.A. 72,* 3536.

Gorovsky, M. A., Yao, M. C., Keevert, J. B., & Pleger, G. L. (1975) *Methods Cell Biol. 9,* 311.

Gorovsky, M. A., Glover, C., Johmann, C. A., Mathis, D. J., & Samuelson, M. (1978) *Cold Spring Harbor Symp. Quant. Biol. 42,* 493.

Greenfield, N., & Fasman, G. D. (1969) *Biochemistry 8,* 4108.

Gross, E. (1967) *Methods Enzymol. 11,* 238.

Isenberg, I. (1977) in *Search and Discovery—a Volume dedicated to Albert Szent-Gyorgi* (Kaimer, B., Ed.) pp 195–215, Academic Press, New York, N.Y.

Isenberg, I. (1978) *The Cell Nucleus 4,* 135.

Johmann, C. A., & Gorovsky, M. A. (1976a) *Biochemistry 15,* 1249.

Johmann, C. A., & Gorovsky, M. A. (1976b) *Arch. Biochem. Biophys. 175,* 694.

Kornberg, R. D. (1974) *Science 184,* 868.

Kornberg, R. D. (1977) *Annu. Rev. Biochem. 46,* 931.

Kornberg, R. D., & Thomas, J. O. (1974) *Science 184,* 865.

Laemmli, U. K. (1970) *Nature (London) 227,* 680.

Mardian, J. K. W., & Isenberg, I. (1978), in press.

Martinson, H. G., & McCarthy, B. J. (1976) *Biochemistry 15,* 4126.

Panyim, S., & Chalkley, R. (1969) *Arch Biochem. Biophys. 130,* 337.

Patthy, L., Smith, E. L., & Johnson, J. (1973) *J. Biol. Chem. 248,* 6834.
Sollner-Webb, B., Camerini-Otero, R. D., & Felsenfeld, G. (1976) *Cell 9,* 179.
Spiker, S., & Isenberg, I. (1977) *Biochemistry 16,* 1819.
Spiker, S., & Isenberg, I. (1978) *Cold Spring Harbor Symp. Quant. Biol. 42,* 157.
van der Westhuyzen, D. R., & von Holt, C. (1971) *FEBS Lett. 14,* 333.
Weintraub, H., Palter, K., & Van Lente, F. (1975) *Cell 6,* 85.
Whittaker, R. H. (1969) *Science 163,* 150.

Exo-Site Affinity Labeling of C1s̄, a Subcomponent of the First Component of Complement, by *m*-[*o*-(2-Chloro-5-fluorosulfonylphenylureido)phenoxybutoxy]benzamidine†

David H. Bing,*‡ Richard Laura, Judith M. Andrews, and Michael Cory

ABSTRACT: Fully activated two chain human C1s̄, a subcomponent of C1̄, the first component of complement, was selectively and irreversibly inactivated with *m*-[*o*-(2-chloro-5-fluorosulfonylphenylureido)phenoxybutoxy]benzamidine [*m*CP(PBA)-F]. The time course of inactivation followed pseudo-first-order kinetics (k_L = 1.52 × 10^{-4} s^{-1}, 23 °C), while the initial rate of inactivation at various inhibitor concentrations followed a rectangular hyperbolic function predicted for affinity labeling kinetics (K_L = 87.3 μM; k_2 = 3.06 × 10^{-3} s^{-1}). The hydrolyzed *m*CP(PBA)-F in which a sulfonic acid replaces the reactive sulfonyl fluoride group was a competitive inhibitor of C1s̄ (K_i = 4.6 μM) implicating active site binding. The analogue *o*-(2-chloro-5-fluorosulfonylphenylureido)methoxybenzene which lacks the active-site-directed benzamidine only slowly inactivated C1s̄ (k_L = 1.35 × 10^{-5} s^{-1}). At a tenfold molar excess of [^{3}H]*m*CP(PBA)-F to C1s̄, 1.078 mol of label was incorporated per mol of C1s̄. Diisopropyl fluorophosphate (Dip-F) and *m*CP(PBA)-OH protected C1s̄ from incorporation of [^{3}H]*m*CP(PBA)-F. In contrast to [^{14}C]Dip-F which labels only the light chain of C1s̄, the [^{3}H]*m*CP(PBA)-F label was distributed 57.6% and 42.3% on the heavy and light chain, respectively. C1s̄ fully inactivated with Dip-F retained the ability to inhibit formation of EAC4,2̄, the cell bound C3 convertase enzyme, whereas *m*CP(PBA)-F inactivated C1s̄ had partially lost this activity. From the dimensions of the *m*CP(PBA)-F reagent we infer the proximity of the heavy chain of C1s̄ to portions of the light chain comprising the catalytic center and suggest that these regions contain those portions on the C1s̄ molecule which specifically bind the complement component C4.

C1s̄[1] is a serine protease which is bound in a Ca(II)-dependent complex with two other proteins C1q and C1r to form C1, the first component of complement. Activated C1s̄ consists of a heavy chain (53 000 daltons) and light chain (29 000 daltons) linked by one or more disulfide bonds. The light chain contains the active site serine within the sequence Ala-Cys-Gly-Lys-Asp-Ser-Gly-Glu(Gly)-Arg. C1s̄ is activated by C1r̄ following the interaction of C1q with immune complexes or other complement activators. The activation proceeds by limited proteolysis of a single polypeptide chain with no apparent decrease in molecular weight. C1s̄ is the enzyme in the C1̄ complex responsible for formation of C3 convertase enzyme via limited proteolysis of the protein substrates C4 and C2 (Reid & Porter, 1975; Cooper & Ziccardi, 1976).

C1s̄ hydrolyzes a number of synthetic substrates. The esters *N*-Ac-Gly-L-Lys-OMe, *N*-Ac-L-Lys-OMe, *N*-Ts-L-Arg-OMe, *N*-Ac-Tyr-OEt, *N*-Z-Lys-ONp, and *N*-Z-L-Tyr-ONp and a tripeptide anilide Boc-Phe-Val-Arg-Na are hydrolyzed (Bing, 1969; Cooper & Ziccardi, 1976; Harpel, 1970; Nagaki & Stroud, 1969; Morgan & Nair, 1977). The turnover rate of these substrates by C1s̄ is very slow compared with the activity of other enzymes such as trypsin, thrombin, and plasmin toward the same compounds (Cooper & Ziccardi, 1976; Morgan & Nair, 1977, Andrews et al., 1978). Like these enzymes, however, C1s̄ is competitively inhibited by substituted benzamidines and phenylguanidine as well as a variety of N-*a*-blocked tyrosines (Bing, 1969; Andrews et al., 1978), further illustrating the hydrophobic and ionic nature of the active site.

The extent to which secondary binding sites define the substrate specificity of C1s̄ is largely unknown. Several studies on the C4 and C2 binding sites in C1̄ have demonstrated competitive inhibition of C2 activity by *N*-Ts-L-Arg-OMe

† From the Center for Blood Research, Boston, Massachusetts, and Wellcome Research Laboratory, Research Triangle Park, North Carolina. *Received June 13, 1978.* Supported by National Institutes of Health Grants AI 14779, AM 17351, HL 18825, CA 17376, and AI 16392.

‡ Recipient of Established Investigatorship of the American Heart Association.

[1] Abbreviations used: Dip-F, diisopropyl fluorophosphate; *m*CP(PBA)-F, *m*-[*o*-(2-chloro-5-fluorosulfonylphenylureido)phenoxybutoxy]benzamidine; *m*CP(PBA)-OH, *m*-[*o*-(2-chloro-5-sulfonic acid phenylureido)phenoxybutoxy]benzamidine; *m*CP(MB)-F, *m*-[*o*-(2-chloro-5-fluorosulfonylphenylureido)methoxy]benzene; *N*-Ac-Gly-L-Lys-OMe, *N*-acetyl-glycyl-L-lysine methyl ester; *N*-Ts-L-Arg-OMe, *N*-tosyl-L-arginine methyl ester; *N*-Ac-L-Tyr-OEt, *N*-acetyl-L-tyrosine ethyl ester; *N*-Z-L-Lys-ONp, *N*-carbobenzyloxy-L-lysine *p*-nitrophenyl ester; *N*-Z-L-Tyr-ONp, *N*-carbobenzyloxy-L-tyrosine *p*-nitrophenyl ester; $NaDodSO_4$, sodium dodecyl sulfate; em, effective molecules; Gdn·HCl, guanidine hydrochloride. The terminology for the complement system is that previously suggested ((1968) *Bull. W.H.O. 39,* 935). The complement components are numbers C1, C2, C4, etc. An activated component is indicated by a line drawn across the top. Thus, C1s̄ is the activated form of the s subcomponent of the first component of complement. EA is sheep erythrocytes sensitized with rabbit anti-sheep erythrocyte antibody. VBS is 0.15 ionic strength Veronal buffered saline, pH 7.4. S-VBS is 0.065 ionic strength VBS made to 300 mosM by addition of sucrose.

0006-2960/78/0417-5713$01.00/0